

High Frequency Linacs for Hadrontherapy*

Ugo Amaldi

*University Milano-Bicocca and TERA Foundation,
Via Puccini 11, I-28100 Novara, Italy
ugo.amaldi@cem.ch*

Saverio Braccini

*Albert Einstein Center for Fundamental Physics and
Laboratory for High Energy Physics
University of Bern
Sidlerstrasse 5, CH-3012 Bern, Switzerland
saverio.braccini@cem.ch*

Paolo Puggioni

*ADAM SA, Rue de Lyon 62,
CH-1211 Geneva, Switzerland
paolo.puggioni@cem.ch*

The use of radiofrequency linacs for hadrontherapy was proposed about 20 years ago, but only recently has it been understood that the high repetition rate together with the possibility of very rapid energy variations offers an optimal solution to the present challenge of hadrontherapy: “paint” a moving tumor target in three dimensions with a pencil beam. Moreover, the fact that the energy, and thus the particle range, can be electronically adjusted implies that no absorber-based energy selection system is needed, which, in the case of cyclotron-based centers, is the cause of material activation. On the other side, a linac consumes less power than a synchrotron. The first part of this article describes the main advantages of high frequency linacs in hadrontherapy, the early design studies, and the construction and test of the first high-gradient prototype which accelerated protons. The second part illustrates some technical issues relevant to the design of copper standing wave accelerators, the present developments, and two designs of linac-based proton and carbon ion facilities. Superconductive linacs are not discussed, since nanoampere currents are sufficient for therapy. In the last two sections, a comparison with circular accelerators and an overview of future projects are presented.

Keywords: Carbon ion therapy; cyclinac; dose delivery; hadrontherapy; linac; medical accelerators; particle therapy; proton therapy.

1. The Challenges Confronting Hadrontherapy

Hadrontherapy, the treatment of tumors with hadron beams, is a new frontier in cancer radiation therapy which is nowadays undergoing rapid development. Since its beginnings, more than 60,000 patients have been treated with protons and light ions in the world [1]. However, about one third of all the patients treated with proton therapy have been irradiated in nuclear and particle physics laboratories by means of nondedicated accelerators. Moreover, less than 2% of all these patients have been treated with pencil beam delivery systems in which

the tumor target is uniformly painted with a large number of successive spots, thus making the best possible use of the properties of charged hadron beams. This fundamental technical advance took place at the end of the last century in two physics laboratories: the Paul Scherrer Institute (PSI; in Villigen, Switzerland), where the spot scanning technique was developed for protons [2], and the Gesellschaft für Schwerionenforschung (GSI; in Darmstadt, Germany), where the raster scanning technique was developed for carbon ions [3]. In 2009 almost all hospital-based centers are still using passive dose delivery systems in which the beam is

*In memory of Mario Weiss, who led the developments of linacs at TERA from 1993 to 2003.

scattered in successive targets and flattened and/or shaped with appropriate filters and collimators [4]. In some centers, the more advanced semiactive “layer stacking” technique is used [5].

In the next few years, hadrontherapy centers must use new approaches to the delivery of the dose if they want to keep pace with the competition of conventional radiotherapy — mainly performed with x-rays produced by electron linacs. Indeed, new techniques have been introduced in the last ten years to conformally cover moving tumors with many crossed beams and spare more and more the surrounding healthy tissues. Many hospitals routinely employ intensity-modulated radiation therapy (IMRT) [6] and are starting to use image-guided radiation therapy (IGRT) [7, 8]. Further improvements have recently been brought by Tomotherapy [9, 10] and rapid arc technologies [11]. Hadron dose delivery systems have to become more sophisticated in order to bring to full fruition the intrinsic advantages of the dose distribution due to a single narrow ion beam characterized, at the end of its range in matter, by the well-known Bragg peak.

Proton beams of energy between 200 and 250 MeV (and very low currents, about 1 nA on target) and carbon ion beams of energy between 3500 and 4500 MeV (and currents of about 0.1 nA on target) are advantageous in the treatment of deep-seated tumors because of four physical properties [12]. Firstly, they deposit their maximum energy density abruptly at the end of their range. Secondly, they penetrate the patient with limited diffusion and range straggling (from this point of view carbon ion beams are about three times better than proton beams). Thirdly, being charged, they can easily be formed as narrow-focused and scanned pencil beams of variable penetration depth, so that any part of a tumor can be accurately irradiated. The fourth physical property is linked to radiobiology and pertains to ions, particularly carbon ions: since each ion leaves in a traversed cell about 24 times more energy than a proton having the same range, the damage produced in crossing the DNA of a cell nucleus is different and includes a large proportion of multiple close-by double strand breaks. This damage cannot be repaired by the usual cell repair mechanisms, so that the effects are qualitatively different from the ones produced by the other radiations; for this reason, carbon ions can control tumors, which

are otherwise radioresistant to both protons and x-rays [13].

The first property is the main reason for using charged hadrons in radiotherapy, since the single beam dose distribution is in all cases superior to that of x-rays, which has an almost exponential energy deposition in matter after a maximum dose delivered only a few centimeters inside the patient’s body. Thus beams of charged hadrons allow in principle a more conformal treatment of deep-seated tumors than beams of x-rays; they give minimal doses to the surrounding tissues, and — in the case of carbon ions — open the way to the control of radioresistant tumors.

The challenge of hadrontherapy is in making full use of the above four properties, especially when the tumor moves, mostly because of the breathing of the patient. The fact that protons and ions have an electric charge, the third property, is the key to any further development but, surprisingly enough, till now practically all therapy beams have been shaped by collimators and absorbers as if hadrons had no electric charge.

In the GSI active “raster scanning” technique, a pencil beam of 4–10 mm width (FWHM) is moved in the transverse plane almost continuously (without switching off the beam) by two bending magnets located about 10 m upstream of the patient. After painting a section of the tumor, the energy of the beam extracted from the carbon ion synchrotron is reduced to paint a less deep layer. In practice, to obtain a variable speed the beam is moved in steps three times smaller than the FWHM of the spot and the next small step is triggered when a predetermined integral of the fluency has been recorded by the ionization chambers placed just before the patient. In this approach the beam is always on.

In the PSI active “spot scanning” technique (which is also called “hold and shoot”), the 8–10 mm (FWHM) spot is moved (switching off the beam) by much larger steps (of the order of 75% of the FWHM of the spot) and, as in the previous case, the transverse movement — which takes about 2 ms — is triggered by ionization chambers measuring the fluence. During the movement of the spot the proton beam extracted from the cyclotron is interrupted for 5 ms by means of a fast kicker.

In both cases the tumor target is painted only once and this is an inconvenience in the case of moving organs, since any movement can cause important

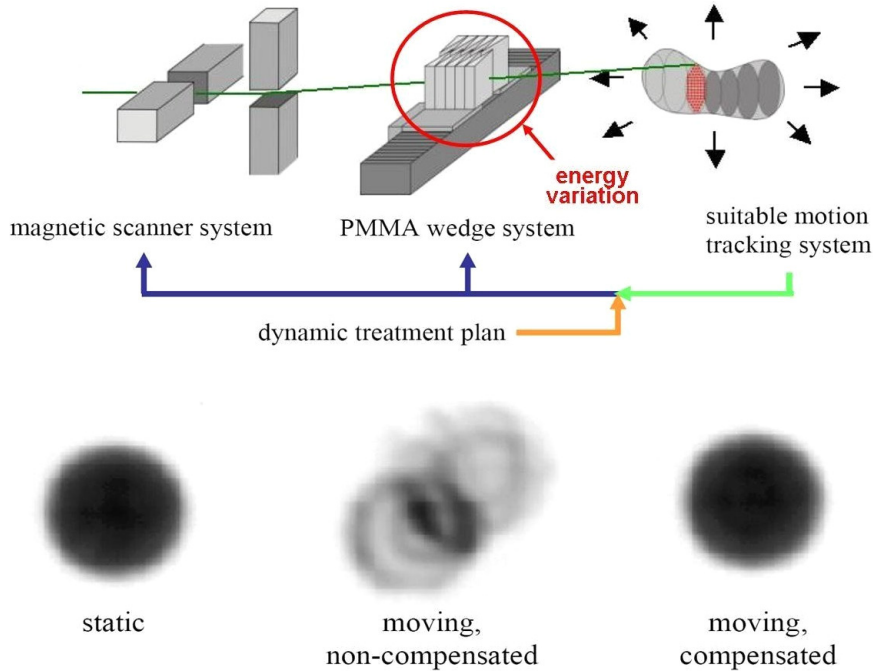


Fig. 1. The feedback system — numerically and experimentally studied at GSI — compensates for the movements of the organs acting, with two bending magnets, to correct the transverse movements and, with absorbers of variable thickness, to compensate for longitudinal movements [14]. (Courtesy of GSI.)

local under- or overdosages. Three strategies have been considered to reduce such effects. In order of increasing complexity, they are:

- (1) In the irradiation of the thorax and the abdominal region, the dose delivery is synchronized with the patient expiration phase in a process called “respiratory gating,” so that the effects on the distribution of the dose due to the movements of the organs are reduced to a minimum (this technique is also used in conventional radiotherapy);
- (2) The tumor is painted many times in three dimensions so that the movements of the organs (if not too large) can cause only small ($\leq 3\%$) overdosages and/or underdosages;
- (3) The movement is detected by a suitable system, which outputs in real time the 3D position of the tumor, and a set of feedback loops compensates for the predicted position in the dose delivery plan with on-line adjustments of the transverse and longitudinal locations of the following spots, as shown in Fig. 1 [14].

An optimal delivery mechanism should be such as to allow the use of any combination of these three

approaches: respiratory gating, multipainting and active angular/energy feedback.

To face these challenges, innovative technological solutions are developed. In this framework, linacs, which are fast-cycling accelerators, offer several advantages and are particularly suited to the multipainting of moving organs, as discussed in Subsecs. 5.2 and 6.1.

2. Linacs Enter Hadrontherapy

This section describes the early design studies of the linacs for proton therapy in a chronological order, from the first proposals in 1989 to the Top-project in 1995.

The focus is on linacs which produce beams directly employed for treating patients, so the developments in the design of hadron low energy linacs used as injectors of medical synchrotrons are not discussed. The reader is referred to the recent papers by U. Ratzinger and collaborators [15, 16].

2.1. The first proton linac for therapy designed at FNAL

The first design of a proton linac for therapy dates back to 1989 [17–19], when at FNAL J. Lennox *et al.*

proposed a hospital-based accelerator for (i) eye treatment with 66 MeV protons, (ii) fast neutron therapy, (iii) boron neutron capture therapy and (iv) isotope production. This multipurpose 24-m-long accelerator had a duoplasmatron H^+ source, a low energy beam transport (LEBT) system, a radiofrequency quadrupole linac (RFQ) and a drift tube linac (DTL) that could deliver up to a $180 \mu A$ average current. The advertised advantages, with respect to the usual approach based on cyclotrons, were the higher dose rate, the limited power costs and the operation in a safer radioactive area.

The RFQ [20, 21] is efficient for very low beta particles ($\beta < 0.06$). The 3 MeV protons were injected into a DTL (consisting of four independent modules) operating at 425 MHz with a low repetition rate (30 Hz) and relatively long pulses ($315 \mu s$). The protons, focused by a system of permanent magnetic quadrupoles (PMQs), could be accelerated at five different energies (3, 7, 27, 47 and 66 MeV) by switching off a certain number of DTL modules. The energy modulation was considered important for obtaining a beam suitable for the applications requiring different proton energies.

2.2. A 3 GHz high repetition rate solution

In 1991, R. Hamm, K. Crandall and J. Potter [22] of Accsys Technology proposed a linac solution composed of three sections. The system is made up of an RFQ–DTL operating at 499.5 MHz, followed by a 3 GHz side-coupled cavity linac (SCL, now called CCL) that accelerates protons from 70 to 250 MeV (Fig. 2). The energy modulation could be achieved by switching off the modules and by using degrading foils. This design was based on a higher frequency (3 GHz), a higher repetition rate (100–300 Hz) and shorter beam pulses ($1\text{--}3 \mu s$) than that of Lennox *et al.*

The high frequency enhances the shunt impedance ($Z \sim f^{1/2}$ [23]) and, for the same power consumption, the total length of the accelerator could be reduced by increasing the mean electric field.

Note that the high repetition rate favors beam scanning while the small output beam size and emittance allow a compact gantry design. The position of the beam can be moved fast (up to 100–300 times in a second) to cover all the area of the treatment. Moreover, the short beam pulses mean an affordable cost of the wall-plug power, because the duty cycle of the RF system (i.e. the repetition rate times the RF effective pulse length) is always smaller than 10^{-3} .

2.3. A 1.28 GHz linac as booster of an existing cyclotron

In 1992, M. P. S. Nightingale *et al.* proposed linear accelerators as boosters of existing hospital cyclotrons, so as to have a cost-effective machine [24]. The 1.28 GHz CCL was designed to boost protons from 62.5 MeV to 200 MeV in about 20 m. The main problem of this structure is the matching with the cyclotron, which usually produces a beam of $50\text{--}300 \mu A$ with large emittance. The Scanditronix MC60 cyclotron of the Clatterbridge hospital, considered in this first study, could be modified to produce a $100 \mu A$ pulsed beam of about $20 \mu s$ with a transverse rms emittance of 9.3π mm mrad, as was demonstrated in 1998 in a study conducted for the TERA Foundation [25].

The design synchronous phase was $\varphi_s = -30^\circ$, so that the longitudinal capture efficiency ($3\varphi_s/360$ [26]) was about 25%. The duty cycle of the RF was set at 0.1%, so that the accelerated average current was about 4×10^3 times smaller than the one injected in the linac.

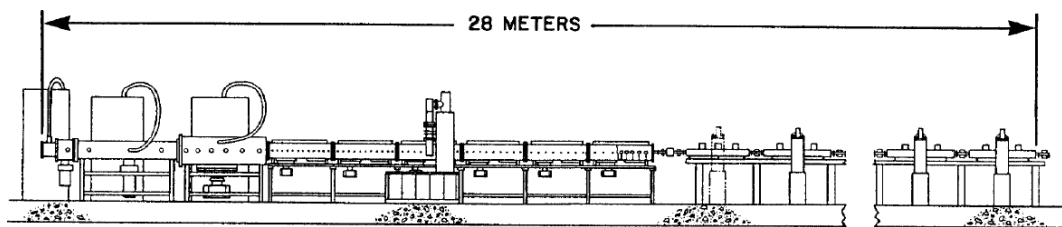


Fig. 2. Schematic layout of the model PL-250 proton therapy linac designed in 1991 by R. Hamm, K. Crandall and J. Potter [22].

The bore radius was calculated so that the FODO structure of the series of PMQs had twice the acceptance of the input emittance ε ; the 70° transverse phase advance guaranteed a minimum β Twiss parameter in each quadrupole [27], so that the transverse physical dimension of the beam ($\sim \sqrt{\varepsilon\beta}$) was smaller than the linac beam hole.

2.4. A traveling wave solution

An innovative approach was proposed by D. Tronc in 1993 [28, 29], when he designed an H-coupled 3 GHz traveling wave (TW) structure. The claim was that this TW linac has higher shunt impedance and a higher quality factor than the classical CCL. By removing the side-coupling cavities, the accelerator has a smaller diameter, so that simultaneous acceleration and focusing become feasible with the introduction of a special external helical focusing [30–32].

In order to get a large Q value and high shunt impedance, the length of the cavities should be as large as possible. This is even more effective at high frequencies (small wavelength λ) and low beta values, when the lengths naturally shrink to maintain the synchronism between the particle and the RF wave. The formula that determines the distance d between the midplanes of two accelerating cavities is

$$d = \frac{\beta\lambda}{2\pi} \Delta\phi, \quad (1)$$

where $\Delta\phi$ is the phase shift between two adjacent cells.

Tronc chose a forward TW linac working in the $-3/4\pi$ mode, which means that $\Delta\phi = (2\pi - 3/4\pi) = 5/4\pi$. Thus, the length of the cavities of this TW linac is larger than that of a CCL that works in the $\pi/2$ mode and has $\Delta\phi = \pi$. According to Tronc's calculations, for $\beta = 0.25$ (30 MeV protons), the shunt impedance of a $-3/4\pi$ TW linac is about 50% higher than for an equivalent CCL structure.

So far, this has been the only attempt to design a TW linac for proton therapy.

The main characteristics of the four approaches described above are listed in Table 1.

2.5. Further designs based on standing wave structures

From 1993 on, and in parallel with the work done for the hadrontherapy center now in construction

Table 1. Characteristics of the four proposals.

Subsection	Type	Freq. (MHz)	Energy (MeV)	Length (m)
2.1	SW	425	0–66	24
2.2	SW	2998	0–250	28
2.3	SW	1280	62–200	20
2.4	TW	2998	0–250	25

in Pavia, the CNAO (Centro Nazionale di Adroterapia Oncologica, Italy [33]), one of us (U. A.) proposed [34, 35] and the TERA group developed a novel type of high frequency and high repetition rate accelerator — a “cyclinac” — which produces charged hadron beams, fulfilling the clinical requirements better than cyclotrons and synchrotrons, as explained in Sec. 8. A cyclinac is an accelerator complex which makes use of a linac as booster of a cyclotron that could be used also for other medical purposes. The study soon branched into two approaches described in the “Green Book [36].”

2.5.1. The cyclinac approach of the TERA foundation

The initial proposal concerned a 30 MeV cyclotron used as injector of a 3 GHz proton linac (Fig. 3). This, as explained above, would imply high gradients and thus a relatively short accelerator.

The choice of the cyclotron energy of the first complete study was dictated by the fact that at 30 MeV the accelerating cells of the first module ($\beta = 0.25$) have very thin separating walls so that the mechanical tolerances and the cooling could be critical. Thus, it was decided that the first CCL would be designed for a 62 MeV input energy, having in mind in particular the cyclotron which is used for eye proton therapy at the Clatterbridge center for Oncology (Liverpool). In 1994 the results of the optimization were presented by M. Weiss and K. Crandall [37], who completed the first design of the linac which in 1998 was dubbed LIBO (LIInac BOoster). The developments which followed are described in Secs. 3, 5 and 6.

2.5.2. The all-linac approach

An all-linac solution was studied by L. Picardi *et al.* for the Top project of ENEA and Istituto Superiore di Sanità (ISS–Rome) [38]. This machine is made up

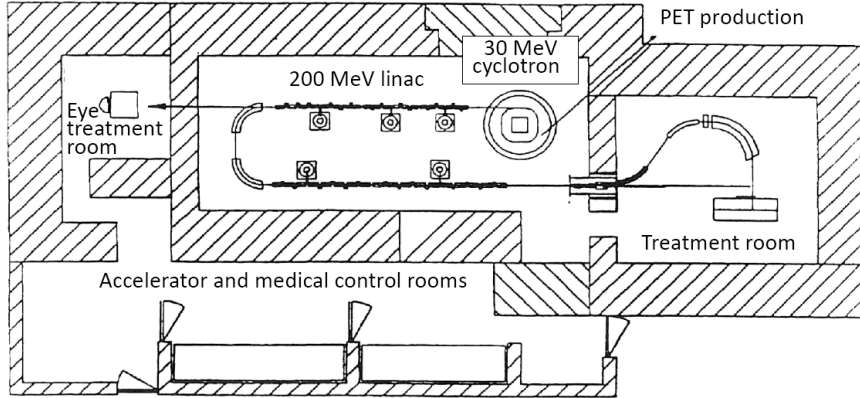


Fig. 3. The first sketch of what was later called a “cyclinac” was based on a 30 MeV commercial cyclotron used also for the production of radiopharmaceuticals [36].

of three sections: (i) an injector (RFQ + DTL) that accelerates protons up to 7 MeV, and (ii) a 3 GHz side-coupled drift tube linac (SCDTL) that injects 65 MeV protons into (iii) a 3 GHz CCL of the LIBO type.

This solution is similar to the one proposed by Hamm *et al.* (Subsec. 2.2), but in the range between 7 and 65 MeV the DTL is replaced by the innovative 3 GHz SCDTL patented in 1995 [39]. In this new structure, a certain number of DTL cavities form a “tank.” The tanks are then coupled by off-axis coupling cavities and oscillate at 3 GHz working in the $\pi/2$ mode.

At low β , this structure has the same high shunt impedance of a DTL (at $\beta = 0.25$ about three times the corresponding one of the CCL) because of the considerable length of the cavities. Moreover, while in a DTL at 3 GHz the gaps between the tubes are so small that there is no space for the PMQs, in the SCDTL the PMQs can be placed on-axis at the location of the coupling cells. At last, the $\pi/2$ operating mode gives great field stability and insensitiveness to tuning errors of the cavities (see Subsec. 3.3). A prototype to accelerate protons from 7 to 11 MeV has been built.

For $\beta \sim 0.34$ (65 MeV protons) the SCDTL shunt impedance decreases and a CCL is the most efficient (see Fig. 16). In the first Top project design, a linear CCL booster accelerated protons from 65 to 200 MeV.

At present the Top IMPLART facility (Intensity-Modulated Proton Linear Accelerator for Radiation Therapy) has been financed for construction at IFO (Istituto di Fisioterapia Ospedaliera, Rome). In this

case the SCDTL structure accelerates protons from 7 to 40 MeV and is followed by the CCL structure described in Sec. 5.

3. Testing of the LIBO Prototype and Recent Developments

For a cyclinac, the fraction of the transmitted beam is in the range 10^{-5} – 10^{-4} . In the case of hadron-therapy, such a minute overall acceptance does not pose any problem because — as remarked above — tumor therapy with protons and carbon ion beams requires beam currents of only 1 nA and 0.1 nA on target, respectively. These very small currents are easily obtained if the linac is placed downstream of a commercial cyclotron capable of producing without problems 10^6 – 10^7 times larger currents. This solution has the added advantage that, if so desired, these high currents can produce in parallel radioisotopes for diagnostics, pain palliation and tumor therapy or be used for research purposes.

Based on these ideas, the 62–200 MeV linac of Ref. 37 was designed in detail and LIBO has been the first prototype of a linac for proton therapy ever built and tested (Fig. 4). This section describes this experience and the ongoing developments.

3.1. The LIBO prototype

In 1998, a collaboration was set up among TERA, CERN (E. Rosso *et al.*), the University and INFN of Milan (C. De Martinis *et al.*) and the University and INFN of Naples (V. Vaccaro *et al.*), with the aim of building and testing the first high frequency proton linac.

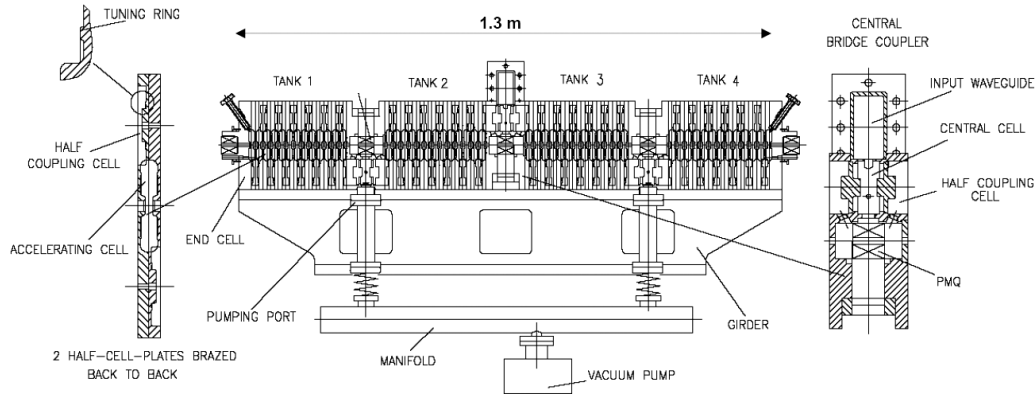


Fig. 4. Mechanical design of the four “tank” of the LIBO prototype, forming one “unit” made up of two “modules.” Each tank is made up of a number of basic units machined with high accuracy in copper and called “half-cell plates.” Permanent magnetic quadrupoles (PMQs) are located between two successive tanks to focus the accelerated proton beam [40].

The LIBO prototype is a 3 GHz side-coupled linac with a design gradient of 15.7 MV/m. As shown in Fig. 4, it is composed of four accelerating tanks, each made one of 23 half-cell plates brazed together. The unit, 1.3m long, is powered through a single central bridge coupler connected to a klystron. During the power tests, performed in the LIL tunnel at CERN, the design gradient was easily reached by injecting the nominal peak power of 4 MW. With the maximum available power from the klystron, a gradient of up to 27 MV/m was reached without discharges [40].

In 2001, the beam acceleration test was performed at the Laboratori Nazionali del Sud of INFN in Catania, by using the LNS Superconducting Cyclotron as injector of LIBO. Protons were accelerated from 62 to 73 MeV, well in agreement with the simulations [41]. The spectrum of the accelerated particles is shown in Fig. 5. Hence, the working

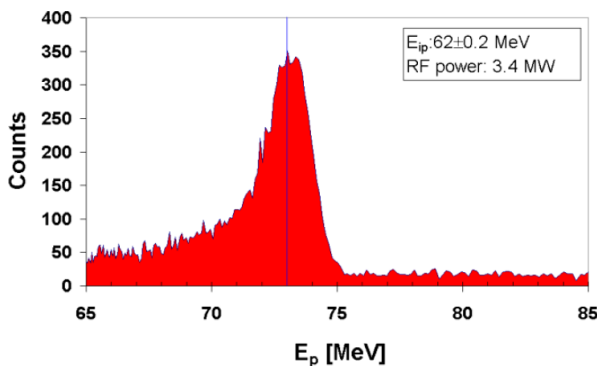


Fig. 5. Proton energy spectrum observed with a NaI crystal located downstream of the LIBO module [41].

principle of a linac as a booster of a cyclotron was completely demonstrated. A paper detailing the tests made and the measurements of the longitudinal acceptance is being completed [41].

3.2. A new design of proton linacs starting from 30 MeV

After the success of the LIBO beam acceleration test at 62 MeV, it was possible to reconsider the initial idea of a 3 GHz proton linac starting from 30 MeV. At this energy the proton speed is about 1.4 times smaller than at 62 MeV and the longitudinal dimensions of the cavities ($d = \beta\lambda/2$, where λ the wavelength of the RF pulse) shrink by the same factor.

In the case of very short cavities ($d = 12$ mm) the cooling, as already said, is more demanding and the machining and the tuning are particularly delicate. Moreover, mechanical tolerances are very tight (better than 10–20 μm) and the measurements of second order coupling effects between the cavities, which could be neglected for higher β and lower frequencies, become critical [42].

Thanks to the use of powerful software for 3D electromagnetic field calculations and the introduction of innovative design procedures [42], the technical problems have been solved and an accelerating module, made up of accelerating cells similar to the ones tested at larger energies, could be built and tested at low power (Fig. 6). These developments are the basis of the linac design which is at present pursued by ADAM SA [43], a CERN spinoff company which is building, for the end of 2009, the

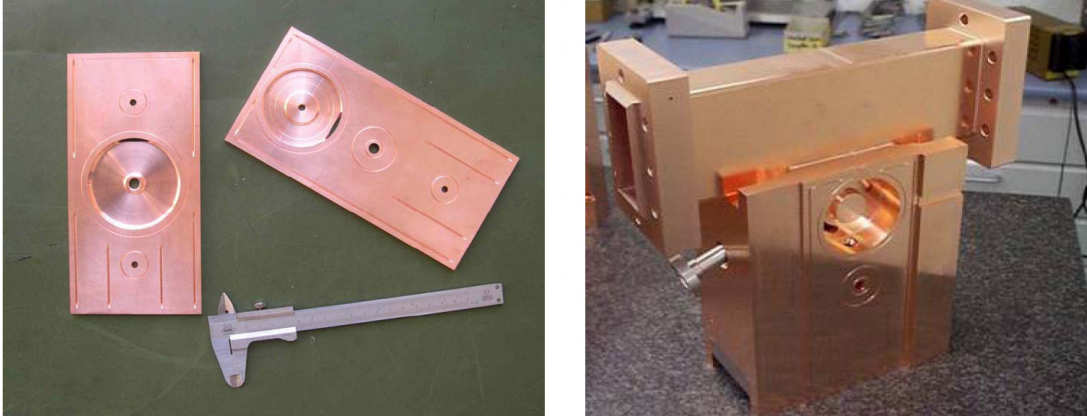


Fig. 6. Two half-cells (left) and the bridge coupler (right) of the 50-cm-long module — made up of two tanks — which accelerates protons from 30 to 35 MeV.

first two modules that accelerate protons from 30 to 41 MeV.

In the last five years the groups led by V. Vaccaro and C. De Martinis have developed a new patented design of the linac plates called a back-to-back accelerating cavity (BBAC) [44]. In the “standard” design of Fig. 6 a tank is made up of identical half-cell plates which exhibit a half coupling cavity on one face and a half accelerating cavity on the other face. The BBAC design foresees instead a portion of an accelerating cavity on one face and the complementary part on the opposite one. The same applies to the coupling cavity. The cutting plane is such as to divide one of the two coupling slots so that the cavities exhibit an asymmetric cut. Therefore one new tile is equivalent to two half-cell plates of the standard design. The main advantages of this solution are:

- The septum between two adjacent cavities is no longer obtained by setting two tiles back to back so that its thickness can be reduced with an increase of the volume/surface ratio and thus of the shunt impedance;
- The reduced number of tiles required to build a tank entails a reduction of the machining and brazing costs.

This design was implemented in the first module of ACLIP, a 3 GHz linac intended to accelerate protons from 30 to 62 MeV. The linac consists of 5 different modules for a total length of 3.1 m [45]. Its first module is made up of 26 accelerating cells arranged

in two tanks. This module was built [46] and power-tested [47] with a 4 MW magnetron/modulator on the premises of the e2v Company (UK) without any indication that the limit of the field gradient had been reached. In autumn 2009, beam acceleration tests will be performed at the Catania INFN-LNS superconducting cyclotron.

These two lines of activities are pursued in Italy in collaboration with CERN, while the studies described in Subsecs. 2.1–2.4 have been discontinued.

4. Standing Wave Linacs for Hadrons

To clarify the most important technical issues, only standing wave (SW) linacs are considered in this section since, as discussed above, among all the design studies of linacs for hadrontherapy which have been performed so far, only one prefigures the use of a traveling wave (TW) structure. TW linacs for electrons have been discussed in Vol. 1 of *Reviews of Accelerator Science and Technology* by P. Wilson [48].

This section is devoted to a short collection of the most important facts and formulae needed in the design of low β SW linacs, with a particular focus on CCL structures.

4.1. RF figures of merit and scaling laws

- *Transit time factor T*. This measures the reduction in energy gain caused by the sinusoidal time variation of the field while the particle is transiting

in the gap. It approaches 1 if the gap between the “noses” of the accelerating cavities is small with respect to $\beta\lambda/2$:

$$T = \frac{\int E(0, z)\cos\omega t(z)dz}{\int E(0, z)dz}. \quad (2)$$

- *Effective shunt impedance per unit of length* ZT . This measures the efficiency of producing an effective axial voltage V_0T for a given dissipated power P per unit of length L :

$$ZT^2 = \frac{(V_0T)^2}{P_0L}. \quad (3)$$

- *Internal quality factor* Q_0 . This takes into account the lossy behavior of the resonator and is proportional to the number of oscillation periods needed to dissipate the energy stored in the cavity:

$$Q_0 = \frac{\omega U}{P_0}, \quad (4)$$

where ω is the resonant frequency, U the stored energy and P_0 the dissipated power. Q_0 is also related to the width of the resonance peak. For a critically coupled cavity [49]:

$$\Delta_H = \frac{2\omega}{Q_0}, \quad (5)$$

where Δ_H is the FWHM of the resonant peak and ω is the resonant frequency.

The shunt impedance scales as $f^{1/2}$, and the quality factor as $f^{-1/2}$. Thus higher frequencies linacs can have the same accelerating gradient consuming less power.

4.2. Figures of merit of the field distribution

- *Field nonuniformity* F_{nu} . It is the relative standard deviation of the fields X stored in the accelerating cavities of a tank:

$$F_{\text{nu}} = \left\langle \frac{\Delta X}{X} \right\rangle_{\text{rms}}. \quad (6)$$

According to the studies of Ref. 50, this parameter is not critical for linac operation. Errors up to $\pm 10\%$ can be accepted without affecting significantly the beam dynamics, provided that the average tank fields, which are determined by the RF power level, are within $\pm 1\%$ of the correct value. However, the requirements for therapy are more stringent. For example, in order to have a precision

of ± 1 mm in the 32 cm water range of 230 MeV protons, the mean energy of the beam must be correct within $\pm 0.2\%$.

- *Power efficiency* ε_p . It is the ratio between the sum of the energy stored in all the accelerating cavities (effective for the acceleration) and the total energy stored in the whole structure:

$$\varepsilon_p = \frac{U_{\text{AC}}}{U_{\text{AC}} + U_{\text{CC}} + U_{\text{BC}}}, \quad (7)$$

where U_{AC} , U_{CC} and U_{BC} are the sum of the energies stored in the accelerating cells (ACs), coupling cells (CCs) and in the bridge coupler (BC), if present, respectively.

4.3. The choice of the $\pi/2$ mode and the stop band

In 1967, Knapp *et al.* [51, 52] demonstrated that the $\pi/2$ mode has many advantages as far as the performance and the stability of the accelerator are concerned:

- Frequency errors of the single cavities affect the frequency and the field distribution of the whole system only through second order effects;
- The losses do not produce any phase shift of the oscillations in the different cavities;
- The spacing between the working frequency and its neighbor modes is larger than in any other mode.

Nowadays, all CCLs work in the $\pi/2$ mode, and also new types of accelerators take advantage of this special mode. For example, structures like SCDTL (discussed in Subsec. 2.5.2) and CLUSTER (discussed in Sec. 7 and in Ref. 53) can accelerate low β particles with greater efficiency and stability than the classical DTL.

In the $\pi/2$ mode, half of the cavities are excited (accelerating cavities, ACs) and half are not (off-axis coupling cavities, CCs). The chain is thus biperiodic, made up of cells with two different geometries and resonant frequencies: ACs and CCs, resonating respectively at ω_a and ω_c . The stop band is the region of frequencies of the dispersion curve (see Fig. 7) in which the structure cannot be excited. It arises when the resonant frequencies of the ACs and CCs do not match.

The stop band is closed only if the following relation is satisfied:

$$\frac{\omega_a}{\sqrt{1-k_a}} = \frac{\omega_c}{\sqrt{1-k_c}}, \quad (8)$$

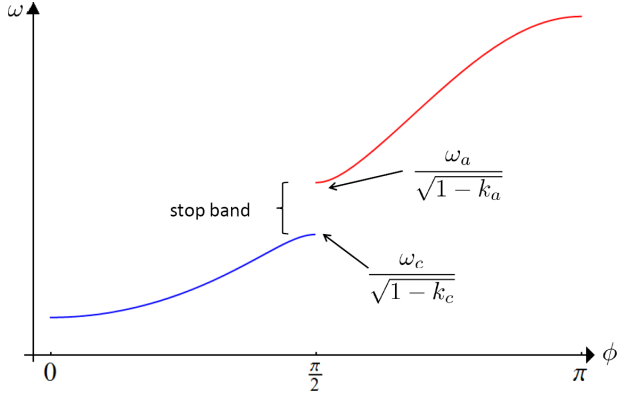


Fig. 7. Dispersion relation of an infinite biperiodic chain (the vertical axis is in arbitrary units). In the stop band no excitation of the structure is possible.

where k_a and k_c are the second order coupling coefficient of ACs and CCs, respectively. As explained in Refs. 51 and 52, in a circuit representation they are proportional to the mutual inductance coefficient between two second neighbor cells. It can be proven that the sensitivity of the system to frequency errors in single cavities is proportional to the amplitude of the stop band. If the stop band is opened, all the advantages of the $\pi/2$ mode vanish.

4.4. Constraints on the number of cavities per tank

In order to minimize the length of the accelerator, to reduce the number of bridge couplers and to lower the power consumption, it is advantageous to have a maximum of accelerating cavities in the same tank.

The energy gain ΔW of a tank is

$$\Delta W = N_c L_c E_0 T \cos \phi, \quad (9)$$

where ϕ is the stable phase [26] and N_c and L_c are the number and the length of the cavities in the tank, respectively. The total power consumption P is given by

$$P = \frac{(E_0 T)^2 N_c L_c}{Z T^2}. \quad (10)$$

By combining Eqs. (9) and (10), the energy gain in a tank of length $N_c L_c$ can be written in the form

$$\Delta W = \sqrt{N_c L_c Z T^2 P} \cos \phi. \quad (11)$$

Thus, for a fixed tank power consumption P , the energy gain is proportional to $N_c^{1/2}$.

However, there are constraints that have to be considered during the design and that limit the

number of cavities per module:

- A structure with N coupled cavities has N resonant modes on the dispersion curve. As N increases, the distance between the $\pi/2$ mode and its neighbors ($\delta\Omega$) decreases [54] as

$$\frac{\delta\Omega}{\omega_{\pi/2}} = k_1 \frac{\pi}{2N}, \quad (12)$$

where k_1 is the first order coupling coefficient, which is the mutual inductance coefficient between two neighbor cavities. Mode-mixing problems may arise if the half width at half maximum Δ_H is approximately as large as $\delta\Omega$. Typical values of the parameters in a 3 GHz CCL for $\beta = 0.25$ are $Q \approx 5000$, $\Delta_H \approx 1.5$ MHz, $k_1 \approx 0.05$, $N \approx 65$, and thus $\delta\Omega \approx 3.5$ MHz.

- The field nonuniformity and the power efficiency deteriorate with increasing N . In Refs. 51 and 52, Knapp *et al.* demonstrate that the field nonuniformity F_{nu} and the ratio $U_{\text{CC}}/U_{\text{AC}}$ are both proportional to N .

4.5. Effects of tuning errors of the ACs and the CCs

Tuning errors of the ACs and the CCs affect the field distribution figures of merit (defined in Subsec. 4.2). The surfaces in Fig. 8 show the values of F_{nu} and ε_p , on the left and on the right respectively, for a given pair of rms errors of ω_a and ω_c .

It is seen that requirements on the precision of ω_a are more critical than those on the precision of ω_c . The power efficiency ε_p is independent of the errors of the CCs, while it is linear in the errors of the ACs. On the other hand, the field nonuniformity F_{nu} depends on the errors of both the ACs and the CCs. However, if the rms error of the ACs is zero, even large errors of the CCs do not change the field distribution.

An error in the resonant frequency of a CC causes the redistribution of the energy stored in the neighbor ACs (affecting F_{nu}) but does not increase the amount of energy stored in the CC itself (ε_p is not affected).

On the other hand, an error on the resonant frequency of an AC increases the field in the neighbor CCs (affecting ε_p) and, at the same time, redistributes the energy stored in that AC and the two neighbor ACs (affecting F_{nu}).

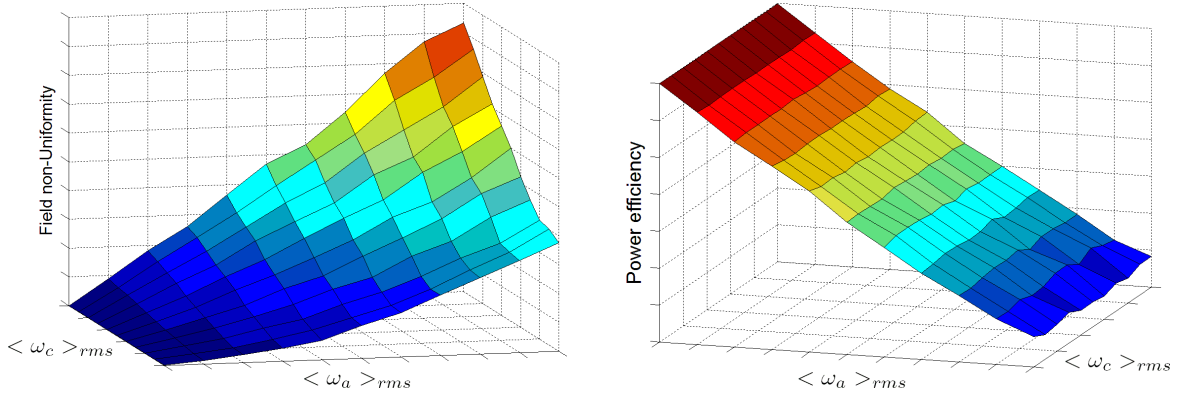


Fig. 8. Qualitative effect of tuning errors on the figures of merit of the field distribution (for the definitions, see Subsec. 4.2). “field nonuniformity” F_{nu} (left) and “power efficiency” ε_p (right). Given a pair of rms errors on ω_a and ω_c , the surface shows the values of F_{nu} and ε_p . All the quantities are in arbitrary units.

The reason for these different behaviors is that, in the $\pi/2$ mode, a very low field is stored in the CCs with respect to the one stored in the ACs.

Relative frequency errors of about 10^{-4} for the ACs (and errors 2–3 times larger for the CCs) are typical requirements for SW linacs.

5. A Linac-Based Facility for Proton Therapy

In 2001, TERA proposed the cyclinac as the heart of a fully fledged multidisciplinary center, named IDRA (Institute for Diagnostics and Radiotherapy) [55]. The main idea of IDRA is to combine on the same site four activities in cancer treatment and research [56]:

- Radioisotope production for diagnostics with PET (positron emission tomography) and SPECT (single photon emission computed tomography),
- Radioisotope production for endotherapy to treat metastasis and systemic tumors,
- proton therapy,
- Research in nuclear medicine and radiation therapy.

IDRA is a physical and cultural space where radiation oncologists, nuclear medical doctors and medical physicists can work together toward the common goal of diagnosing and curing solid tumors and their metastases with both teletherapy and endotherapy techniques.

The main features of IDRA are:

- A 30 MeV high current commercial proton cyclotron with several external beams,

- Various 30 MeV high current beams for isotope production and research,
- a high gradient side-coupled linac — based on the LIBO prototype — which accelerates protons from 30 to 230 MeV with a continuous range of energies,
- One or more treatment rooms equipped with fixed beams and/or rotating gantries for the treatment of deep-seated tumors.

5.1. The linac of IDRA

The parameters of the linac are summarized in Table 2. An artist’s view of IDRA featuring an eye therapy beam and three gantries is shown in Fig. 9 [57, 58]. In only 18 m, 30 MeV protons are accelerated up to 230 MeV. The high repetition rate (100–200 Hz) makes this linac particularly suitable for the spot scanning technique (Subsec. 5.2).

The small effective duration of each RF pulse ($3.2 \mu\text{s}$) determines the 150 kW total plug power. The difference between the effective duration of the RF pulse and the duration of the proton pulse ($1.5 \mu\text{s}$) is due to the filling time of the structure: $Q_0/2\omega$.

The effective shunt impedance per unit of length is low for the first modules (about $30 \text{ M}\Omega/\text{m}$), as the CCL is not efficient for low- β particles, but then rises to $90 \text{ M}\Omega/\text{m}$ at the end of the linac. With such impedances, the needed overall RF peak power is 60 MW, which can be provided by 10 compact modulator/klystron systems similar to the one shown in Fig. 10. These modulators are robust commercial solid state devices which, in case of failure, can within 2–3 h be easily exchanged as a single unit with their klystron.

Table 2. Main parameters of LIBO [58].

Accelerated particles	p^{+1}
Type of linac	CCL
RF frequency (MHz)	2998.5
Input energy (MeV)	30
Output energy (MeV)	230
Total length of the linac (m)	18.5
Cells per tank/tanks per module	16/2
Number of accelerating modules	20
Thickness of a half cell in a tank (mm)	6.3–14.6
Diameter of the beam hole (mm)	7.0
Normalized transversal acceptance (mm mrad)	1.8π
Number of permanent magnetic quadrupoles	41
Length of each PMQ (mm)	30
PMQ gradients (T/m)	130–153
Synchronous phase (deg)	-15
Peak power per module (with 20% losses) (MW)	3.0
Effective shunt impedance ZT^2 (inj.-extr.) (M Ω /m)	30–90
Axial electric field (inj.-extr.) (MV/m)	15–17
Number of klystrons (peak power = 7.5 MW)	10
Total peak RF power for all the klystrons (MW)	60
Klystron RF efficiency	0.42
Repetition rate (Hz)	≤ 200
Duration of a proton pulse (μ s)	1.5
Max. number of protons in 1.5 μ s (2 Gy L $^{-1}$ min $^{-1}$)	$4 \cdot 10^7$
Effective duration of each RF pulse (μ s)	3.2
RF duty cycle	$3.2 \cdot 10^{-4}$
Plug power at 100 Hz + 100 kW auxiliaries (kW)	150

This accelerator complex presents many advantages with respect to the currently used proton therapy machines (see Sec. 8). The dose delivery can

naturally be performed by active methods in all three dimensions. The transversal coordinates of the beam are controlled by the use of bending magnets, while the longitudinal one is determined by continuously and rapidly varying the energy of the beam. If each module is powered by one klystron, the depth of the Bragg peak can be changed by selecting the number of active klystrons and by adjusting the power sent to the last active one. Thus, as shown in Fig. 11, a continuous range of energies is achieved and the penetration depth can be varied in only 2 milliseconds in steps of ± 1 mm. This is obtained by rapidly adjusting only the low power signals of the drivers of the klystrons.

In the design of Table 2, to reduce the number of modulator/klystron systems, each of those powers two modules at the same time. This still allows one to rapidly vary the energy in the 90–230 MeV range.

5.2. Dose delivery and multipainting techniques with protons

In radiation therapy, a $\pm 2.5\%$ uniform dose has to be delivered to the tumor target. To obtain such uniformity using the spot scanning technique, the optimal distance between the spots is calculated from their natural FWHM. As already mentioned, in the PSI spot scanning technique [2] the distance is 75% of the FWHM so that the dose nonuniformity is smaller

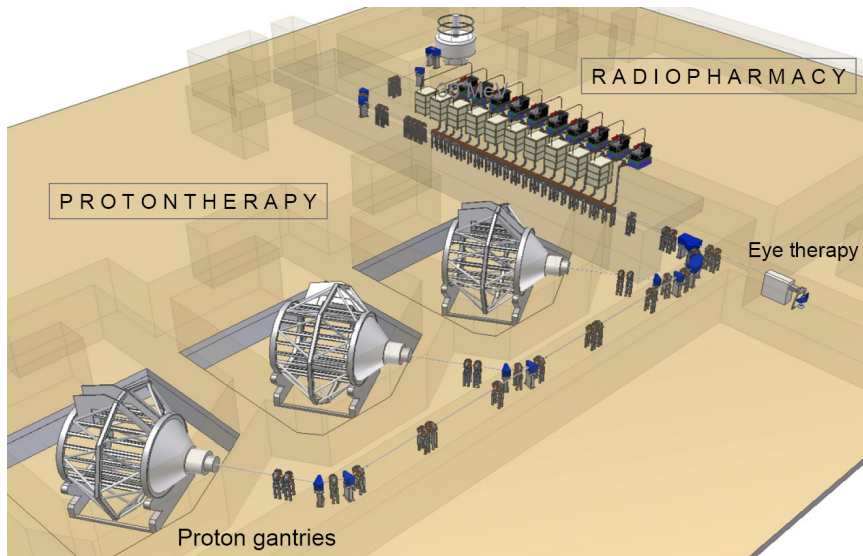


Fig. 9. A typical layout of IDRA features a 30 MeV cyclotron, a linac of the LIBO type and three treatment rooms equipped with rotating gantries and a fixed beam line for the treatment of eye tumors [58].



Fig. 10. The 7.5MW klystron is powered by a solid state modulator commercialized by ScandiNova Systems AB (Uppsala). LIBO employs 10 modulator/klystron systems.

than $\pm 1.25\%$. In the GSI raster scanning method the distance is 30% of the FWHM and the tumor is painted only once without switching off the beam in between the “visits” to the 2.5 denser voxel lattice. A pulsed cyclinac beam can be used both ways in

conjunction with a 3D feedback system, but for the treatment of moving organs, as discussed at the end of Sec. 1, spot scanning with multipainting is preferred. The reasons are that both systematic errors in the delivered dose average out when the same voxel is visited more than 10 times and, if a spot is missing, which corresponds to a 3% drop of the local dose, the error can be corrected during the next paintings.

At a 200 mm water depth the natural lateral spread of the Bragg peak has an FWHM of 11.5 mm, which, combined with a proton pencil beam having an FWHM of 7 mm, gives an overall FWHM of 13.5 mm. This corresponds to a 6.4 mm lateral falloff (80%–20%), which has to be compared with the 5.5 mm “natural” value. Figure 12, taken from Ref. 58, shows the relative number of protons to be stopped in each voxel so as to uniformly irradiate from a single direction and with “almost round” spots a 1 L volume (diameter = 12.4 mm). The number of protons peaks at the distal edge, because the front slices are crossed by the beams reaching deeper voxels. The figure is just an example, since in a real treatment more directions will be used, in particular when employing the linac variable beam energy to implement the very effective “distal edge tracking” technique (DET) [59].

A 12-times painting of a moving organ with spots containing a number of protons (adjusted

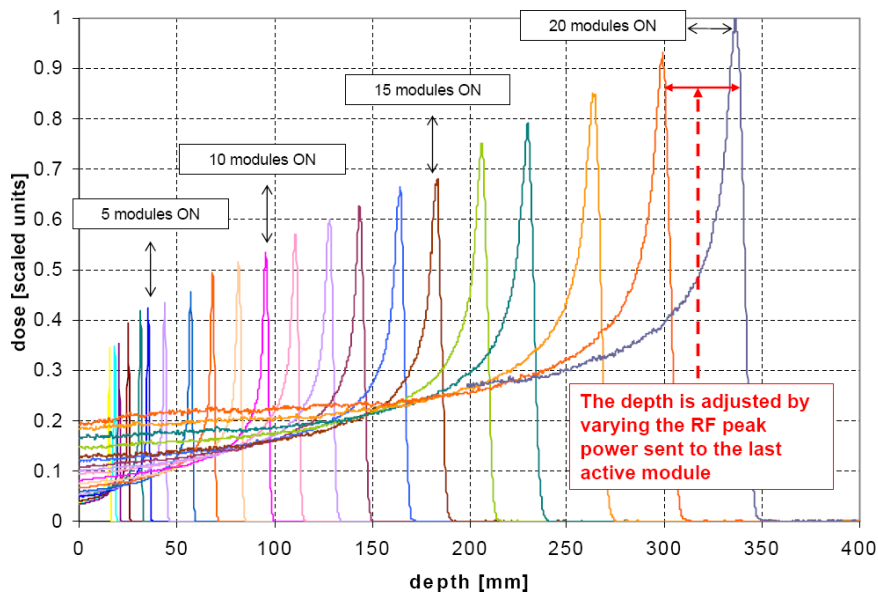


Fig. 11. Proton depth dose distribution when the number of the active accelerating modules is varied one by one. To avoid superpositions a different normalization is used for each curve [58].

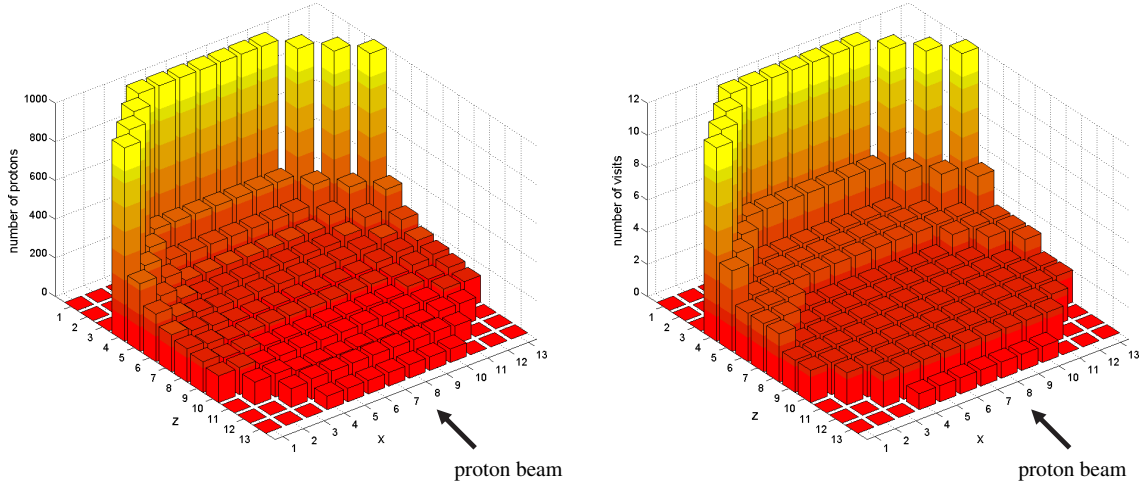


Fig. 12. Number of protons (in arbitrary units) delivered in each voxel of the central transversal slice needed to obtain a $\pm 1.25\%$ uniform dose distribution to a 6.2-cm-radius spherical volume (1 L) centered at a 20 cm depth in water (left); number of “visits” needed to obtain a flat equivalent dose distribution with the condition that any missing visit dose not change the total local dose by more than 3% (right). The coordinates z and x are given as a number of voxels; z is the longitudinal and x the transversal coordinate [58].

by controlling the cyclotron source) which fluctuate from one visit to the next by $\pm 5\%$ implies a $\pm 1.5\%$ effect on the dose accuracy. The right panel of Fig. 12 shows that the proximal voxels need many less visits so that, on average, each spot is painted 3.5 times [58]. Table 2 shows that the maximum number of protons in a spot needed to deliver, at 100 Hz, the $2 \text{ Gy L}^{-1} \text{ min}^{-1}$ standard dose is $N_m = 4 \cdot 10^7$. By taking into account the linac overall transmissions, this corresponds to a $150 \mu\text{A}$ current from the cyclotron, which is 3–5 times smaller than the one routinely produced by commercial 30 MeV cyclotrons. Of course, when sending one of the cyclotron beams to the linac, the source will be chopped at the linac repetition rate so to minimize the activation of the components.

6. A Linac-Based Facility for Carbon Ion Therapy

In 2004, TERA designed a LIBO-like structure to postaccelerate carbon ions having 300 MeV/u, such as those produced by the superconducting cyclotron designed by L. Calabretta *et al.* of the LNS-INFN laboratories in Catania and dubbed SCENT (Superconducting Cyclotron for Exotic Nuclei and Therapy) [60,61]. The working principle of CABOTO (CARbon BOoster for Therapy in Oncology) is similar to that of LIBO. High frequency (3 GHz), high repetition rate (≤ 400 Hz) and short hadron

Table 3. Parameters of the carbon ion Linac.

Accelerated particles	C ⁺¹
Type of linac	CCL
RF frequency (MHz)	2998.5
Input energy (MeV/u)	300
Output energy (MeV/u)	430
Total length of the linac (m)	22
Cells per tank / tanks per module	15/2
Number of accelerating modules	16
Thickness of a half cell in a tank (mm)	15–18
Diameter of the beam hole (mm)	8
Normalized transversal acceptance (mm mrad)	2.8π
Number of permanent magnetic quadrupoles	33
Length of each PMQ (mm)	60
PMQ gradients (T/m)	140–170
Synchronous phase	-15°
Peak power per module (with 25% losses) (MW)	4.5
Effective shunt impedance ZT^2 (inj.-extr.) (M Ω /m)	100–110
Axial electric field (inj.-extr.) (MV/m)	25–23
Number of klystrons (peak power = 7.5 MW)	16
Total peak RF power for all the klystrons (MW)	75
Klystron RF efficiency	0.42
Repetition rate (Hz)	≤ 400
Duration of a carbon ions pulse (μs)	1.5
Max. number of C ions in $1.5 \mu\text{s}$ ($2 \text{ Gy L}^{-1} \text{ min}^{-1}$)	$1.6 \cdot 10^5$
Effective duration of each RF pulse (μs)	3.2
RF duty cycle	$1.3 \cdot 10^{-3}$
Plug power at 400 Hz + 100 kW auxiliaries (kW)	330

pulses ($1.5 \mu\text{s}$) are the main characteristics of this 22-m-long linac for carbon ions, which is particularly suited for the spot scanning technique with multipainting [62].

The most relevant parameters of a recent version of CABOTO are collected in Table 3. It has to be underlined that in this case the ion source is a critical component since, to obtain the maximum number of carbon ions in a visit $N_m = 1.6 \cdot 10^5$, when the transmissions of the cyclotron and the linac are taken into account, the source has to deliver in $1.5 \mu\text{s}$ about $1.6 \cdot 10^5$ fully stripped ions at 400 Hz [58]. Such intensity can be produced by the new superconducting Electron Beam Ionization Sources (EBIS) produced by DREEBIT GmbH (Dresden) [63].

Carbon ions can be accelerated from 300 up to 430 MeV/u in a continuous range of energies by selecting the number of “active” modules and modulating the energy by changing the input power in the last active module, as already discussed for IDRA.

A scheme of the dual carbon ion and proton center designed by G. Cuttone *et al.* is shown in Fig. 13. The installation of the 16 accelerating modules of CABOTO will be a second phase of the facility which is planned for the Cannizzaro Hospital in Catania [64]. In the first phase, the 17 cm water range of 300 MeV/u carbon ions will allow the treatment of 85% of all head and neck tumors and 80% of all lung and liver tumors [62].

It is worth noting that the carbon ion linac is shorter than the standard transport lines present in every center to bring the hadrons from the accelerator to the treatment rooms.

6.1. Dose delivery and multipainting with carbon ions

The dose delivery system is based on the spot scanning technique, used also for LIBO, but it has to take into account the different behavior of carbon ions with respect to protons. As a matter of fact, the Bragg peak produced by carbon ions is sharper and the lateral falloff is smaller than the proton one. For instance, the natural FWHM of the spot produced at 20 cm by a 330 MeV/u carbon beam is 3.1 mm, almost 4 times narrower than that of protons having the same range. By using a pencil beam with an FWHM of 5 mm, the overall transverse value of the FWHM is 5.9 mm, corresponding to a 2.8 mm falloff, to be compared with the 1.5 mm natural one. Longitudinally the FWHM is intrinsically smaller than 5.9 mm, but the unique property of the linac beam comes to the rescue: by slightly varying the proton energy, when visiting 12 times the same voxel, the Bragg peak can be widened as needed. With the same

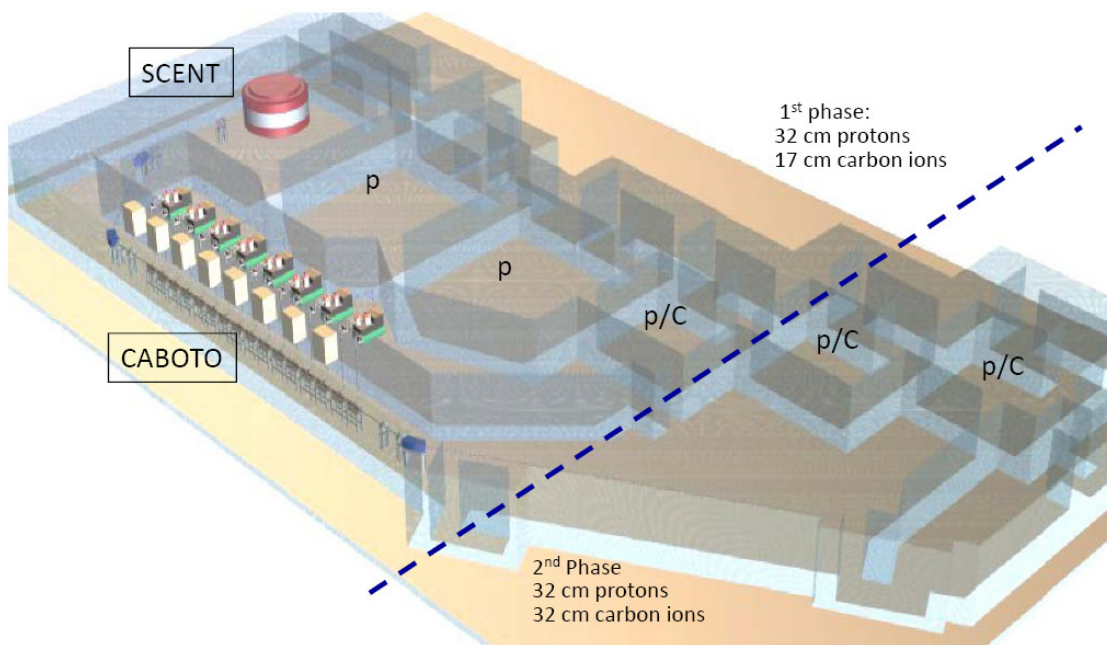


Fig. 13. The hadrontherapy center designed by the Catania group is the one schematically shown on the left of the blue line. The installation of the line will allow reaching with carbon ions a water depth of 32 cm in the rooms on the right of the blue line.

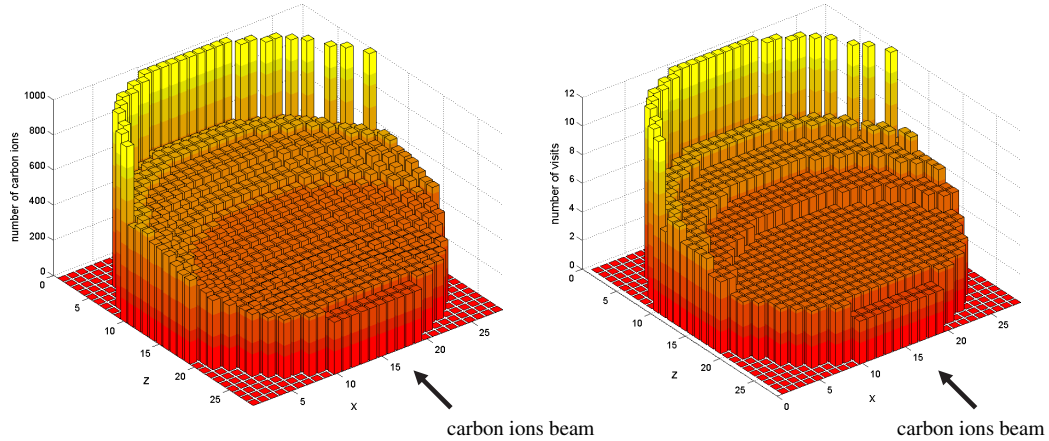


Fig. 14. Number of carbon ions (in arbitrary units) delivered in each voxel of the central transversal slice needed to obtain a $\pm 1.25\%$ uniform biological dose distribution to a 6.2 cm-radius spherical volume (1 L) centered at a 20 cm depth in water (left); number of “visits” needed to obtain a flat dose distribution with the condition that any missing visit dose not change the dose by more than 3% (right). The coordinates z and x are given as a number of voxels; z is the longitudinal and x the transversal coordinate. With respect to protons, due to the smallest FWHM of the beam, the number of spots for each dimension is double [58].

PSI criterion adopted for proton scanning, the distance between the spots is set at 75% of the overall FWHM and the number of voxels needed to cover the 1 L sphere is easily obtained.

The two histograms of Fig. 14 and the value $N_m = 1.6 \cdot 10^5$ needed to deliver $2 \text{ Gye L}^{-1} \text{ min}^{-1}$ (Table 3) have been computed by taking into account the fact that the “physical dose” is different from the “equivalent dose,” which is calculated by multiplying the physical dose by the effective local RBE (relative biological effectiveness) [65]. This semiempirical parameter takes into account the relative effectiveness (with respect to the x-rays) of the carbon ions in causing lethal damage to the cells. Since for carbon ions the RBE is typically 1.5 at the beginning of the path inside the tissue and increases to about 3 at the very end of the range, the physical dose delivered to the distal slices of the tumor target has to be lower than the one delivered in the middle in order to obtain a “flat” equivalent dose.

7. CLUSTER, an Innovative Low β H-Type Structure

If the linac has to accelerate carbon ions having an energy definitely smaller than 100 MeV/u, the relatively low shunt impedance of CCL structures implies a further increase of the power consumption.

The need for high power efficiency in the low β range (0.05–0.3) leads to the choice of H-mode

accelerating cavities, also called TE cavities because the electric field is naturally directed transversally with respect to the structure axis. These structures have been studied since 1950 [66, 67] and are nowadays used at low frequencies (100–200 MHz) at GSI [68] and in Linac3 at CERN [69].

H-mode cavities are drift tube cavities operating in the $H_{n1(0)}$ mode, where the index n is usually 1 (IH cavities; already existing) or 2 (CH cavities, under development). These cavities are very attractive because of the high shunt impedance for low β particles due to the fact that the generally transverse electric field is made parallel to the axis and concentrated in the accelerating gaps by the metallic drift tubes. Moreover, they are π -mode structures, i.e. the RF accelerating field is phase-shifted by 180° between successive gaps, a feature allowing higher average gradients, which in the present case are further increased by the choice of a large frequency (3 GHz).

In 2003, the TERA Foundation designed and patented a new type of H-mode accelerator that is particularly suitable for high frequencies and low β . The concept of CLUSTER (Coupled-cavity Linac Using Transverse Electric Radial field) is to connect a certain number of H-mode tanks, by using special bridge couplers, in a single resonant structure operating in the $\pi/2$ mode, as shown in Fig. 15. This choice is the novelty of this design and gives great stability to the field at these high frequencies (see

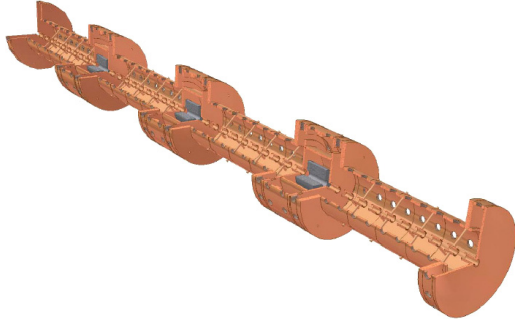


Fig. 15. Module of CLUSTER, the Couple-cavity Linac Using Transverse Electric Radial field. The accelerating tank consists of a sequence identical (constant β) accelerating units, each formed by an accelerating gap and two half drift tubes. The accelerated beam is focused by PMQs [53].

Subsec. 4.3). In order to further increase the shunt impedance, at 3 GHz the tanks consist of CH cavities, while, at lower frequencies, classical IH cavities could also be adopted. The coupling cell of the bridge couplers resonates in the TEM_{011} mode and their geometrical dimensions have been chosen so that the PMQs can be positioned on axis [53, 70].

In Fig. 16, the efficiency of this structure is compared with the approaches discussed in the previous sections. This interesting low β , high frequency and high shunt impedance structure can be adapted to many applications:

- (1) High current proton acceleration at 500–700 MHz for radioisotope production using a linac system;
- (2) Low current booster for proton therapy, to be used, for instance, in an IDRA center (see Sec. 5) that features an 18 MeV cyclotron and needs a linac capable of accelerating $\beta = 0.2$ protons;

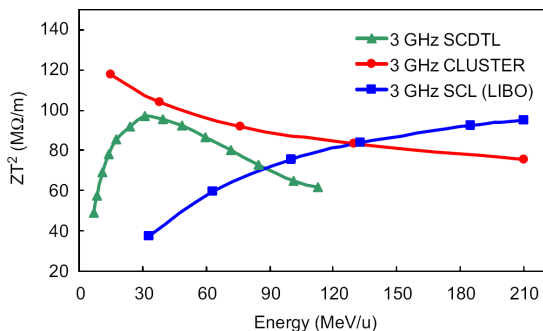


Fig. 16. Effective shunt impedance for three 3 GHz linacs, with a 2.5 nm iris radius: LIBO, SCDTL, CLUSTER [53].

- (3) Low current booster for carbon ions, in a center having, for instance, a 60 MeV/u cyclotron ($k = 250$) as injector of the linac.

8. Linacs and Circular Accelerators: A Comparison

At present, all the hadrontherapy centers in operation or under construction are based on circular accelerators: cyclotrons and synchrotrons. For proton therapy both solutions are in use and commercial companies offer complete centers based on one or the other technology. On the other hand, due to the larger energy and magnetic rigidity, synchrotrons are employed to accelerate carbon ions. Only recently has it been announced that the first prototype of a superconducting cyclotron for protons and carbon ions will be built by the company IBA [71].

As far as the size is concerned, proton cyclotrons — normal or superconducting — have 4–5 m diameters while proton synchrotrons have 6–8 m diameters. For carbon ions the diameters of the synchrotrons are in the range 19–25 m.

The beam produced by cyclotrons is characterized by a fixed energy — usually in the range from 230 to 250 MeV for protons — and a 30–100 MHz pulsed beam which can be considered continuous when compared with the human respiration period. This kind of beam is surely suited for coping with the organ motion problem but needs a quite long special device installed in the beam line — usually called ESS, for “energy selection system” — which varies the beam energy by mechanically moving absorbers in times of the order of 100 ms and, downstream of the absorbers, requires a set of quadrupoles, bending magnets and slits to select the energy and “clean” the lower energy beam. The ESS hall becomes a radioactive area due to beam losses — especially if 60–70 MeV energies are used for eye treatments. Due to fragmentation, this system represents an even more critical issue for carbon ions.

The beam produced by synchrotrons is characterized by a spill time of about 1 s, during which the beam is extracted for therapy, and by a filling and accelerating time of about 1–1.5 s in which the beam is not available. From spill to spill the energy can be varied as one wishes even if, in case of passive scattering, only a few energies are usually commissioned and used. It has to be noted that the beam periodicity is similar to that of the respiration cycle,

Table 4. Properties of the beam of various accelerators.

Accelerator	The beam is always present?	The energy is electronically adjusted?	Which is the approx. time (in ms) to vary E_{\max} ?
Cyclotron	Yes	No	100
Synchrotron	No	Yes	1000
Linac	Yes	Yes	1

which represents a disadvantage for the irradiation of moving organs with the “gating” technique.

As shown in Table 4, the beam produced by linacs presents several advantages with respect to both cyclotrons and synchrotrons and it can be considered as optimal for applications in hadrontherapy. Linacs are in fact completely flexible in their capability of varying both the energy and the intensity of the beam in 1–2 ms.

In a cyclinac, the energy can be varied between the cyclotron output value and the maximum possible for the linac, but this feature will never be used because of the finite momentum acceptance of the beam transport channel. However, a $\pm 1.5\%$ momentum acceptance is sufficient to obtain a very fast adjustment ΔR of the particle range: $\Delta R/R \approx \pm 5\%$. This corresponds to a longitudinal fast adjustment of ± 10 mm for an $R = 200$ mm. For deep-seated tumors, this is more than enough to compensate for the longitudinal variation of the particle path in the patient’s body due to organ movements.

For tumors located at a 50–70 mm depth, the ± 3 mm fast adjustment may not be enough, but the range variation can be more than doubled by using larger energies and a 10 cm absorber located very close to the patient.

This possibility can be combined with the standard use of two transverse magnetic fields and allows the use of a fast and electronically controlled 3D feedback system. This system acts on the power levels of the last active klystron to vary the energy, and on the intensity of the cyclotron source to adjust the number of particles delivered in the next spot. The absence of passive absorbers and mechanical devices is surely advantageous in terms of reliability, maintenance and radiation protection.

Particle beams accelerated by linacs have many features in common with the ones produced by (non-scaling) fixed field alternating gradients accelerators (FFAGs), which are, typically, high current accelerators but have recently been designed for producing

the nanoampere proton [72] and carbon ion beams [73] needed in radiation oncology. It has to be noted that nonscaling FFAGs have not yet been built, their RF systems are complicated and the extraction of a variable energy beam is difficult. On the contrary, high frequency linacs are very common, their RF systems are commercial items and beam extraction poses no problem.

9. Very High Gradient Linac Structures and Future Developments

The natural yardstick for measuring a medical linac is the 15–20 m length of the ESS needed for reducing the energy of the proton and carbon ion beams extracted from cyclotrons. The designs of Tables 2 and 3 have these lengths, and new approaches to shortening them are certainly worthwhile. Moreover, if shorter linacs could be produced, one could build “single room facilities” in which a proton linac rotates around the patient, as described in the patent of Ref. 74 under the name TULIP, which stands for “TURNing LINac for Proton therapy.”

The first limitation on the miniaturization of hadron linacs is power consumption, which — for a given total acceleration voltage — increases proportionally to the electric field and — fixing also the field — is inversely proportional to the length [Eqs. (9)–(11)]. A second limitation comes from electron field emission (FE) with the consequent breakdown phenomena — which can locally destroy the metal surface.

In the 1950s, Kilpatrick assumed that destructive breakdowns happen when FE is enhanced by a cascade of secondary electrons ejected from the cathode by ion bombardment [75]. A simple calculation led to the Kilpatrick criterion, which states that the limiting surface electric field increases roughly as the square root of the RF frequency. With the data available at the time, the Kilpatrick field at 3 GHz was computed to be $E_{\max} = 49$ MV/m. In the following years, structures were built in which the maximum surface field was twice the Kilpatrick field.

In the last 20 years, in connection with the design of normal conducting electron–positron colliders in the 10–30 GHz range, many more data have been collected which show that (i) the phenomena are complicated and ions do not play an important role [48], (ii) at 3 GHz the limit is definitely larger

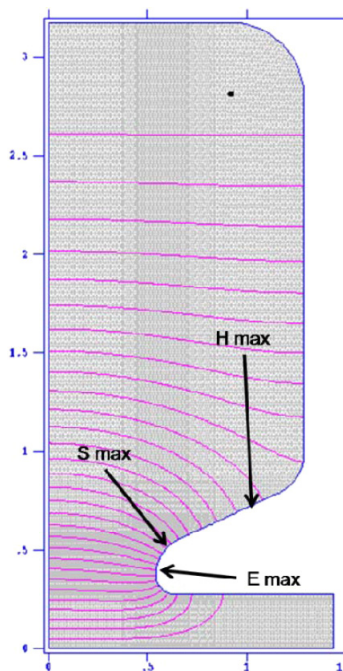


Fig. 17. The red curves represent the electric field lines of the accelerating mode and the arrows indicate the regions of a typical CCL accelerating cavity where the Pointing vector S and the electric and magnetic fields (E , H) are maximal.

than 150 MV/m [76], and (iii) E_{\max} is roughly constant above about 15 GHz [77]. Recently, at CERN, a new quantity has been introduced — the “modified Poynting vector,” [78] which has been shown to determine the breakdown rate. This new understanding has opened the way to the design of shorter high frequency linacs for hadrontherapy.

In an SW cavity such as the one in Fig. 17, the ratio between the maximum field E_{\max} and the accelerating field in the gap can be varied in the range 5–8, so that at 3 GHz accelerating gradients as large as 30 MV/m can be obtained. At larger frequencies the gradient can be further increased, so since 2008 TERA and the CLIC RF structure group at CERN led by W. Wuensch have been collaborating on the design of new 9–12 GHz structures.

The development of larger gradient structures finds its limit in the power consumption, which, for a given repetition rate, is proportional to the duration of the RF pulse. In the case of SW linacs this duration cannot be reduced below a couple of microseconds because of the filling time of the structure, which at 3 GHz is about $1.5 \mu\text{s}$ (Subsec. 5.1). TW linacs do not have this limitation and are thus good

candidates for short hadron linacs running at frequencies larger than 3 GHz.

Acknowledgments

The financial support of the Monzino Foundation (Milano), the Price Foundation (Geneva), the Associazione per lo Sviluppo del Piemonte (Torino) and Accelerators and Detectors for Medical Applications — ADAM SA, Geneva — is gratefully acknowledged.

References

- [1] Particle Therapy Cooperative Group (PTCOG), <http://ptcog.web.psi.ch/ptcenters.html>
- [2] E. Pedroni, R. Bacher, H. Blattmann, T. Böhringer, A. Coray, A. Lomax, S. Lin, G. Munkel, S. Scheib, U. Schneider and A. Tourosvsky, *Med. Phys.* **22**, 37 (1995).
- [3] T. Haberer, W. Becher, D. Schardt and G. Kraft, *Nucl. Instrum. Methods A* **330**, 296 (1993).
- [4] A. M. Koelher *et al.*, *Med. Phys.* **4**, 297 (1977).
- [5] N. Kaematsu *et al.*, *Med. Phys.* **29**, 2823 (2002).
- [6] S. Webb, *Intensity-Modulated Radiation Therapy* (Institute of Physics Publishing, Bristol and Philadelphia, 2001).
- [7] D. A. Jaffray, *Semin. Radiat. Oncol.* **15**, 208 (2005).
- [8] G. Baroni, M. Riboldi, M. F. Spadea, B. Tagaste, C. Garibaldi, R. Orecchia and A. Pedotti, *J. Radiat. Res.* **48**, A61 (2007).
- [9] T. R. Mackie *et al.*, *Med. Phys.* **20**, 1709 (1993).
- [10] www.tomotherapy.com
- [11] F. Lagerwaard, W. Verbakel, E. van der Hoorn, B. Slotman and S. Senan, *Int. J. Radiat. Onc. Biol. Phys.* **72**, S530 (2008).
- [12] U. Amaldi and G. Kraft, *Rep. Prog. Phys.* **68**, 1861 (2005).
- [13] H. Tsujii *et al.*, *J. Radiat. Res.* **48**(Suppl.), A1 (2007).
- [14] S. Goetzinger *et al.*, *Phys. Med. Biol.* **3**, 34 (2008).
- [15] H. Vormann, B. Schlitt, G. Clemente, C. Kleffner, A. Reiter and U. Ratzinger, Status of the linac components for the Italian hadrontherapy center CNAO, in *Proc. EPAC08* (2008), pp. 1833–1835, and references therein.
- [16] U. Ratzinger, G. Clemente, C. Commenda, H. Liebermann, H. Podlech, R. Tiede, W. Barth and L. Groening, A 70 MeV proton linac for the FAIR facility based on CH-cavities, in *Proc. LINAC 2006* (2006), pp. 526–530.
- [17] A. J. Lennox, F. R. Hendrickson, D. A. Swenson, R. A. Winje and D. E. Young, Proton linac for hospital-based fast neutron therapy and radioisotope production. Fermi National Accelerator Laboratory, TM-1622 (1989).

- [18] A. J. Lennox, *Nucl. Instrum. Methods B* **56/57**, 1197 (1991).
- [19] A. J. Lennox and R. W. Hamm, A compact proton linac for fast neutron cancer therapy, in *Proc. Acc. Tech.* (Long Beach, California, 1999), pp. 33–35.
- [20] T. P. Wangler, *Principles of RF Linear Accelerators* (John Wiley and Sons, 1998), pp. 225–257.
- [21] I. M. Kaochinskiy and V. A. Teplakov, *Prib. Tekh. Eksp.* **2**, 12 (1970).
- [22] R. W. Hamm, K. R. Crandall and J. M. Potter, Preliminary design of a dedicated proton therapy linac, in *Proc. PAC90*, Vol. 4 (San Francisco, 1991), pp. 2583–2585.
- [23] Ref. 20, p. 50.
- [24] M. P. S. Nightingale, A. J. T. Holmes and N. Griffiths, Booster linear accelerator for proton therapy, in *Proc. LINAC92* (Ottawa, 1992), pp. 398–401.
- [25] J. A. Clarke *et al.*, Assessing the suitability of a medical cyclotron as an injector for an energy upgrade in *Proc. EPAC98* (Stockholm, 1998), pp. 2374–2376.
- [26] P. Lapostolle and M. Weiss, Formulae and procedures useful for the design of linear accelerators, CERN-PS-2000-001 (2000), available at <http://preprints.cern.ch>
- [27] Ref. 20, pp. 209–210.
- [28] D. Tronc, *Nucl. Instrum. Methods A* **327**, 253 (1993).
- [29] D. Tronc, Compact protontherapy unit design, in *PAC93* (1993), pp. 1768–1770.
- [30] D. Tronc, Patent F 91 09292.
- [31] D. Tronc, Patent F 92 06290.
- [32] D. Tronc, Patent F 93 03152.
- [33] U. Amaldi and G. Magrin (eds.), *The Path to the Italian National Center for Ion Therapy* (Mercurio, Vercelli, 2005).
- [34] U. Amaldi, The Italian hadrontherapy project, in *Hadron Therapy in Oncology*, eds. U. Amaldi and B. Larsson (Elsevier, 1994), p. 45.
- [35] U. Amaldi and G. Tosi, The hadron therapy project three years later. TERA 94/13, GEN 11.
- [36] M. Weiss *et al.*, *The RITA Network and the Design of Compact Proton Accelerators*, eds. U. Amaldi, M. Grandolfo and L. Picardi (INFN, Frascati, 1996), Chap. 9.
- [37] K. Crandall and M. Weiss, Preliminary design of a compact linac for TERA. TERA 94/34, ACC **20**, (1994).
- [38] L. Picardi *et al.*, Progetto del TOP Linac. ENEA-CR, Frascati (1997), RT/INN/97-17.
- [39] L. Picardi, C. Ronsivalle and A. Vignati, Struttura SCDTL. Patent No. RM95-A000564.
- [40] U. Amaldi, P. Berra, K. Crandall, D. Toet, M. Weiss, R. Zennaro, E. Rosso, B. Szeless, M. Vretnar, C. Cicardi, C. De Martinis, D. Giove, D. Davino, M. R. Masullo and V. Vaccaro, *Nucl. Instrum. Methods A* **521**, 512 (2004).
- [41] C. De Martinis *et al.*, Acceleration tests of a 3 GHz proton linear accelerator (LIBO) for hadron therapy. To be submitted to *Nucl. Instrum. Methods A*.
- [42] P. Puggioni, Radiofrequency design and measurements of a linear accelerator for hadrontherapy, Thesis, Milano-Bicocca University (2008).
- [43] www.adam-geneva.com
- [44] V. G. Vaccaro, Patent No 2008 A25.
- [45] V. G. Vaccaro *et al.*, ACLIP: a 3 GHz side coupled linac to be used as a booster for 30 MeV Cyclotrons, in *Proc. Cycl.* (2007), pp. 172–174.
- [46] V. G. Vaccaro *et al.*, Design, construction and low power RF tests of the first module of the ACLIP linac, in *Proc. EPAC08* (2008), pp. 1836–1838.
- [47] V. G. Vaccaro *et al.*, RF high power tests on the first module of the ACLIP linac, in *Proc. PAC09* (2009).
- [48] P. B. Wilson, Electron linac for high energy physics, in *Reviews of Accelerator Science and Technology*, Vol. 1, 2008, pp. 7–42.
- [49] S. Turner (ed.), *CAS* (CERN accelerator school), Ch. 2. CERN Yellow Reports (1992).
- [50] G. R. Swain, R. A. Jameson, E. A. Knapp, D. J. Liska, J. M. Potter and J. D. Wallace, *IEEE Trans. Nucl. Sci.* 614 (1971).
- [51] E. A. Knapp, B. C. Knapp and D. E. Neagle, *Rev. Sci. Instrum.* **38–11**, 1583 (1967).
- [52] E. A. Knapp, B. C. Knapp and J. M. Potter, *Rev. Sci. Instrum.* **39-7**, 979 (1968).
- [53] U. Amaldi, A. Citterio, M. Crescenti, A. Giuliacci, C. Tronci and R. Zennaro, *Nucl. Instrum. Methods A* **579**, 924 (2007) and arXiv:physics/0612213.
- [54] Ref. 20, p. 112.
- [55] U. Amaldi *et al.*, Institute for Advanced Diagnostics and Radiotherapy — IDRA. TERA note, 2001/6 GEN 31 (July 2001).
- [56] R. Zennaro, *ICFA Beam Dynam. Newslett.* **36**, 62 (2005).
- [57] U. Amaldi, S. Braccini, A. Citterio, K. Crandall, M. Crescenti, G. Magrin, C. Mellace, P. Pearce, G. Pitta, E. Rosso, M. Weiss and R. Zennaro, Cyclinacs: fast-cycling accelerators for hadron therapy, [arXiv:0902.3533v1 (2009)].
- [58] U. Amaldi, S. Braccini, M. Crescenti, G. Magrin, C. Mellace, P. Pearce, G. Pitta, P. Puggioni, E. Rosso, M. Weiss and R. Zennaro, Accelerators for hadron therapy: from Lawrence cyclotrons to linacs. To be published in *Nucl. Instrum. Methods A* (2009).
- [59] U. Oelfke and T. Bortfeld, *Technol. Cancer Res. Treat.* **2-5**, 401 (2003).
- [60] L. Calabretta and M. Maggiore, Study of a new superconducting cyclotron to produce a 250 MeV — 50 kW light ion beams, in *Proc. EPAC02* (Paris, France, 2002), pp. 614–617.

- [61] L. Calabretta, G. Cuttanea, M. Maggiore, M. Rea and D. Rifuggiato, *Nucl. Instrum. Methods A* **562**, 1009 (2006).
- [62] U. Amaldi, Cyclinacs: novel fast-cycling accelerators for hadron therapy, in *Proc. Cycl. 2007* (2008), pp. 166–168.
- [63] G. Zschornack, F. Grossmann, V. P. Ovsyannikov and E. Griesmayer, Dresden EBIS-SC: a new generation of powerful ion sources for the medical particle therapy, in *Proc. Cycl. (2007)*, pp. 298–299.
- [64] G. Cuttone, private communication.
- [65] M. Scholz and G. Kraft, *Radiat. Prot. Dosimetry* **52**, 29 (1994).
- [66] P. Blewett, Linear accelerator injector for proton synchrotrons, in *Proc. High Energy Accelerators and Pion Physics* (Geneva, 1956).
- [67] P. M. Zeidlitis and V. A. Yamnitskii, *J. Nucl. Energy, Part C* **4**, (1962).
- [68] U. Ratzinger, The new GSI prestripper linac for high current heavy ion beams, in *Proc. LINAC96* (CERN, Geneva, 1996), pp. 288–292.
- [69] N. Angert, W. Bleuel, H. Gaiser, G. Hutter, E. Malwitz, R. Popescu, M. Rau, U. Ratzinger, Y. Bylinski, H. Haseroth, H. Kugler, R. Scrivens, E. Tankle and D. Warner, The IH linac of the CERN lead injector, in *Proc. LINAC94* (Tsukuba, Japan, 1994), pp. 743–746.
- [70] U. Amaldi, M. Crescenti and R. Zennaro, Linac for ion beam acceleration. US Patent 6888326.
- [71] Y. Jongen, presented at PTCOG 47 (Jacksonville, USA, May 2008).
- [72] D. Trbojevic, A. G. Ruggiero, E. Keil, N. Neskovic and A. Sessler, Design of a non-scaling FFAG accelerator for proton therapy, in *Proc. Cycl. 2004* (2005), pp. 246–248.
- [73] E. Keil, A. M. Sessler and D. Trbojevic, *Phys. Rev. ST Accel. Beams* **10**, 054701 (2007).
- [74] U. Amaldi, S. Braccini, G. Magrin, P. Pierce and R. Zennaro, Ion acceleration system for medical and/or other applications. Patent WO 2008/081480 A1.
- [75] W. P. Kilpatrick, *Rev. Sci. Instrum.* **28**, 824 (1957).
- [76] J. W. Wang and G. A. Loew, Field emission and RF breakdown in high-gradient room-temperature linac structures. SLAC PUB 7684 (Oct. 1997).
- [77] W. Wuensch, High-gradient breakdown in normalconducting RF cavities. EPAC02 (2002), pp. 134–138.
- [78] A. Grudiev and W. Wuensch, A new local field quantity describing the high gradient limit of accelerating structures, in *Proc. LINAC08* (Victoria, Canada, 2008), pp. 936–938.

Ugo Amaldi as staff of Italian National Health Institute (ISS, Rome) in the 60s worked in radiation physics and opened two lines of research: $(e, e'p)$ in nuclei and $(e, 2e)$ in atoms. In 1973 he moved to CERN where he co-discovered the rise of the hadronic cross-sections with energy, published the first paper proposing a high-energy superconducting linear collider, founded and directed for 13 years the DELPHI collaboration at LEP and published a paper about the supersymmetric unification of the fundamental forces, which has more than 1200 citations. From the end of the 80s he has taught particle and medical physics in the two Milan Universities. In 1992 he created the TERA Foundation to design the Italian national carbon ion facility CNAO, which is being commissioned in Pavia, and to apply linac technologies to hadrontherapy. More than one third of the Italian high-school pupils study physics on his textbooks.

Saverio Braccini is a senior physicist at the Laboratory for High Energy Physics of the University of Bern where he leads the research activities on medical applications of particle physics. He was formerly Technical Director of the Foundation for Oncological Hadrontherapy TERA, where he contributed to the development of innovative accelerators and detectors for the treatment of tumours with hadron beams. Previously, he has been active in particle physics at the Large Electron Positron Collider (LEP) and at the Large Hadron Collider (LHC) at Cern, giving important contributions to low energy QCD and to the construction of high precision particle detectors.

Paolo Puggioni is a young physicist graduated in Milano-Bicocca University with Prof. U. Amaldi. In the last two years his research activity focused on radiofrequency design, measurements and beam dynamics of low current linacs for hadrontherapy. He is a collaborator of the TERA Foundation and of ADAM SA, a CERN spin-off company in the medical accelerator business. At the moment he is completing his postgraduate studies in Neuroinformatics at the Edinburgh University.